Synergy Estimation Method for Simultaneous Activation of Multiple DOFs Using Surface EMG Signals

Rabya Bahadur[1,2], Saeed ur Rehman[1], Ghulam Rasool[3], Muhammad A. U. Khan[4]

[1]Sir Syed CASE Institute of Technology, Islamabad, Pakistan.
[2]COMSATS UI, Abbottabad Campus, Pakistan.
[3]Rowan University, NJ, USA.
[4]Namal Institute, Mianwali, Pakistan.

Abstract

Surface electromyography signals are routinely used for designing prosthetic control systems. The concept of synergy estimation for muscle control interpretation is being explored extensively. Synergies estimated for a single active degree of freedom (DOF) are found to be uncorrelated and provide better results when used for single movement classification; however, an increase of simultaneously active DOFs leads to complex limb movements and multiple DOF detection becomes a challenge. Synergy estimation is a non-convex optimization technique, this paper proposes the use of regularized non-negative matrix factorization for the estimation of synergistic weights during complex movements. The use of regularization constraint makes the overall problem bounded and provide smoothness by avoiding overfitting. The proposed technique showed better accuracy when tested for activation of multiple DOF simultaneously at a significantly lower computational time, i.e., by 34%.

Keywords: Electromyography; Synergy; Kalman filter; Non-negative Matrix Factorization

Introduction

Myoelectric control refers to the translation of surface electromyography (sEMG) signals as a stimulus for assistive device control. It presents countless possibilities in neuro-rehabilitation and human-machine interface applications [1]. Currently, there are three active sEMG strategies in the research community, namely, pattern recognition (PR) based systems [2-4], synergy based systems [5-8], and a hybrid system based on the merger of the two [9,10]. A generalized block-diagram based comparison for all the three categories is presented in fig. (1). PR has been extensively explored in the past two decades for sEMG and provides better results in terms of percentage accuracy and online data analysis [11]. However, despite its advances regarding accuracy level when multiple positions or multiple force levels are involved, there is a considerable decrease in the performance of PR based classifiers [4]. To address this shortcoming, robust classifier requires an extensive workload in the training phase [1]. This limitation bounds PR based classifiers from commercial use leaving the stage open for conventional state machine-based systems. Alternatively, research and understanding of synergistic muscle activation in the past decade has led many to believe that synergy-based models are more viable solution for commercial use [1,8,9].

The sEMG is a composition of time-varying motor unit action potentials transmitted to the spinal cord via nerves [1,12]. The control signals from the spinal cord are translated into a group of time-varying muscle signals through a set of time-invariant discrete weights (referred to as synergies) [11,13,14]. The investigation by Santello et al., suggests that there exists a strong correlation among different gripping postures of the hand [15]. Two synergies (i.e., the first two principal components) provide information about almost 80% of all gripping postures. Thus, an effective estimation of these synergies holds the key to simultaneous and proportional control.

Hahne et al., utilize the concept of co-adaptation of human as well as time-invariant synergies by providing visual feedback in the "close-loop system" [16]. The study activates two DOFs (for the upper arm) simultaneously and estimates the effect of visual feedback for estimation of movements using a linear regressor. The study provides a proof of concept with very encouraging results, but the adopted methodology is very time consuming (i.e., an average delay of 400 msec to 1 sec), whereas the nominal duration should be around 120 msec at maximum [17]. Lin et al., propose the use of Non-negative Matrix Factorization (NMF) with sparseness constraint for the extraction of bases information for multiple DOF control [18]. One of the main constraints for NMF based time-invariant synergy estimation is the extraction of sequential bases using a single DOF. Thus, training with each single active DOF is a compulsion that can later be extended to multiple DOFs. Lin et al., claim that the maximization of sparseness constraint with NMF obtaining optimal bases and single DOF calibration is not a necessity anymore. The retrieved results are compared with classic NMF as well as regression-based synergy systems. However, it is a known fact that sparseness-based solutions are not unique and the extraction of a convergent solution is not guaranteed [19]. Therefore, the synergies estimated can affect the discrimination of tasks and thus, performance.
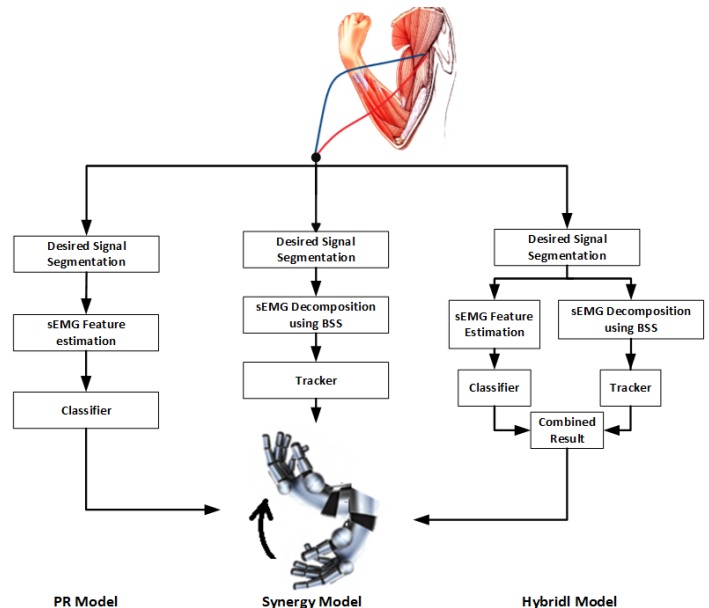

Figure 1 sEMG: surface electromyography; PR: pattern recognition; BSS: blind source separation; the figure

presents a generalized comparison of three methodologies; namely, PR Model, Synergy Model and Hybrid Model.

In addition to PR and synergy-based systems, there also exist some hybrid models that provide a blend of both. The paper proposed by Zhang et al., formulate a combination of PR and synergy estimation-based system for the classification of active DOFs, one dedicated for each finger [10]. The variance accounted for (VAF) test results in the selection of 11 synergies for classification purposes. The high dimensionality and dedication of one DOF classifier for each finger (a total of five classifiers), as well as two synergy estimators dedicated for each classifier makes the complete process computationally exhaustive. Rasool et al., propose the use of probabilistic independent component analysis (pICA) for synergy estimation with preliminary results cross verified by applying a linear discriminant analysis classifier [9]. The work is tested for both online and offline analysis. Current paper is inspired by Rasool's paper and the results of the proposed work are compared with his work for offline processing using the same dataset.

Synergies estimated for single DOF are found to be uncorrelated and leads to better hand posture identification results [20]. However, complex limb movements involve the activation of multiple DOFs simultaneously. Decoding sEMG for complex tasks is therefore a challenge and a topic for active research. This paper advocates the use of an efficient synergy model for identification of hand postures based on single and double DOF activation. The results are based on offline analysis. The proposed work recommends the use of regularized NMF to obtain optimal synergy weights. The estimated synergy weights are then employed by Kalman filter as a system model. A preliminary study of the proposed model for the detection of single DOF achieving an accuracy of 97.6 to 99.5% was presented earlier in a conference paper [20].

The rest of the paper is organized as follows. The paper initially addresses experimental setup, the mathematical model is explained in detail in the next section; correlating the central nervous system (CNS) as a stochastic process, followed by synergy estimation technique. Experimental setup is described in the later part followed up by results and discussion. The conclusion is presented at the end of the paper.
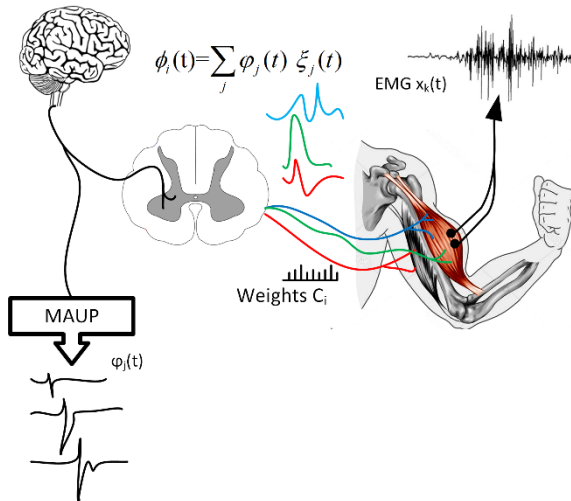

Figure 2: The detail of the sEMG formation.
Figure 3 The given diagram provides a detail of the sEMG formation, i.e., the control signals $\varphi_j(t)$ in the form of impulses are issued from the brain. At the spinal cord, multiplicative noise $\xi_j(t)$ is introduced. The spinal cord signals form a superimposed combination of the control signals and weights as presented by the equation $\phi_i(t) = \sum_j \varphi_j(t)\xi_j(t)$. When transmitting the signal to the appropriate muscle the neuro-muscular system adds weights $C_{k,i}$. A convoluted and noisy version of the weighted control commands is observed by the kth muscle, i.e. sEMG, $x_k(t)$

Experimental Setup

The sEMG data were collected from 12 healthy participants after approval by the ethical review committee and written informed consent of the participants was obtained. Each participant performed two sets of movements, the first set comprised of activation of only a single DOF at one time, i.e., movements involving wrist flexion and extension, wrist supination and pronation, and hand opening and closing. The second set consisted of eighteen movements in total involving simultaneous activation of two DOFs combining the above-mentioned movements. In our data recording, each movement was performed for 5 sec with a rest of 5 sec between such movements. A total of 8 sEMG electrode sets were placed in a symmetrical manner around the forearm. sEMG data were recorded using AgCl electrodes with Noraxon TeleMyo Direct Wireless Transmission System, which had inbuilt filtering of 10-500 Hz. The data was digitized using NI-USB 6009 acquisition unit with a sampling frequency of 2000 samples per second. For a detailed description of the experimental setup refer to the paper [9].

Mathematical Model

This mathematical model is built on the premise that after planning voluntary movements in the CNS, appropriate commands (referred to as the control signals $\phi_j(t)$) are issued to relevant skeletal muscles through motor neurons via the spinal cord and peripheral nervous system. On receiving these neural commands, the skeletal muscles get activated to accomplish the task. These activations are modulated by changing the number of recruited motor units (and thus muscle fibers) and their firing rate [21]. The control signals transmitted from the spinal cord are modeled as $(t) = [\phi_1(t), \phi_2(t), \ldots, \phi_J(t))]^T$, where J is the total number of active DOF for the current task. A visual description of the flow of information in the CNS from the motor cortex to the targeted muscle; is presented in fig. 2. It is important to note that the noise in the CNS (i.e. $\xi_j(t)$) is multiplicative by nature, not additive and is directly proportional to the control signal ($\varphi_j(t)$) issued for the jth DOF by the CNS [22].The signal received at the kth muscle, $x_k(t)$, is the sum of product of the control signals ($\varphi_j(t)$), multiplicative noise $\xi_j(t)$ and weights assigned ($C_{k,i}$, as a result of cross-talk between the kth and i^{th} muscle):

$$x_k(t) = \sum_i C_{k,i} \sum_j \varphi_j(t)\xi_j(t), \qquad (1)$$

$$y_l(t) = h_{l,k}(t) * x_k(t) + e(t), \qquad (2)$$

where $h_{l,k}(t)$ is the transfer function of the medium between the lth electrode and k^{th} muscle (i.e., skin, fat, and non-contractile tissue), '$*$' represents convolution and $y_l(t)$ is the recorded sEMG signal while $e(t)$ represents the environmental artifacts and noise. The signal recorded through sEMG electrodes is a convoluted sum of muscle signals with the additive noise of the environment.

In the matrix form it can be expressed as:

$$X(t) = Z\phi(t) \tag{3}$$

Where $X(t) = [x_1(t), x_2(t), ..., x_K(t))]^T$, bold face capital letters represent matrices while small letters are representing vectors. $Z \in \mathbb{R}^{[K \times J]}$ represents the internal synergy weight matrix added by the neuro-muscular system and indicates the extent to which the kth muscle is participating in the activation of the jth DOF. The complete system multiplier model is represented by $S = HZ$, a product of internal synergy matrix 'Z' with external filtering effects of skin and electrode 'H'. An estimation of the synergy matrix 'S' using the recorded sEMG provides a link to the neural control commands. Synergy estimation problem transforms into a blind source separation problem defined as:

$$Y(t) = HZ\,\phi(t) + E(t)$$
$$= S\phi(t) + E(t) \tag{4}$$

where, sEMG signal is represented as $Y(t) = [y_1(t), y_2(t), ..., y_K(t))]^T$; and synergy matrix, $S \in \mathbb{R}^{[L \times J]}$ and $E \in \mathbb{R}^{[L \times 1]}$.

State Space Model for the CNS

The CNS can be modeled as a noisy dynamic system using state-space formulation. The complete system can be represented as a dynamic system followed up by measurement model. State-space formulation allows the employment of optimal Bayesian filtering for the estimation of the unknown state of the system, i.e., command signals transmitted from the spinal cord. The state-space model translated the state variable, x_t (control signals, $\phi(t)$) to the state observer (sEMG signal), given as

$$x_t = x_{t-1} + n_{1,t}, \tag{5}$$
$$y_t = sx_{t-1} + n_{2,t}, \tag{6}$$

where x_{t-1} represent the system state at time $t-1$, y_t is the output of the system, i.e., the sEMG. Whereas $n_{1,t}$ and $n_{2,t}$ represents process and measurement white Gaussian noise with zero mean and known co-variance matrices Q and R, respectively.

The system's dynamic model captures the temporal behavior of the evolution of control signals or the system state x_t and is modeled using the random walk process. The observation or the measurement model maps the system state to the system outputs y_t, i.e., voltage levels recorded using the sEMG electrodes. The measurement model is defined using the muscle synergies, i.e., $s \epsilon S$ which relates the system state x_t to the system output y_t.

Estimation of Muscle Synergies

The recorded sEMG signals $Y(t)$ is a composition of the control signals distributed from spinal cord ($\phi(t)$), and weights introduced by the neuro-muscular system of the body (S), both are unknown quantities and formulates to be a blind source separation problem. As an exact solution does not exist in such

a case; therefore, approximation methods are adopted where the objective is to minimize the estimated error, $E(t)$, by decomposing the sEMG matrix into control signals and synergistic weights, as:

$$E = Y(t) - S\phi(t) \tag{7}$$

An estimation of muscle synergy matrix (S) makes the state-space model completely defined. In the proposed paper synergy matrix 'S' is estimated for various hand movements followed by employment of Kalman filter to track the control commands, issued by the spinal cord. A detailed explanation of the proposed methodology is given in (Fig. 3).
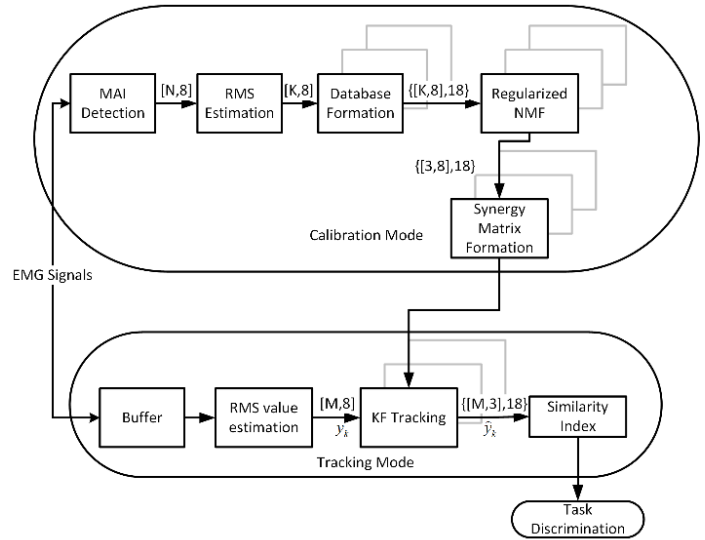

Figure 4: The proposed model in two stages.
Figure 5 The figure describes the proposed model in two stages. Stage one is referred to as Calibration Mode where task specific synergies are estimated using regularized NMF. The second stage namely, Tracking mode, employees Kalman filter for the tracking of the associated task using the sEMG signals. As we are taking 8 channel sEMG recording; thus, we have RMS values of $[N \times 8]$, where N is the length of MAI interval and 'r' is the rank of the state observer matrix.

Blind source separation algorithms employed in the past generally belong to two main categories, i.e., independent component analysis (ICA) [9,23,24] and NMF [18,25,26]. One of the major drawbacks of ICA or any of its variants is the requirement of independence of the source channels, something which is hard to establish for biological systems; thus, other decomposition algorithms that do not require independence pre-assumptions are explored. One decomposition of interest is NMF [5,6,14,16,18,26]. NMF decomposes the provided observer matrix into two matrices with the property that all three matrices are non-negative. Both the decomposition matrices, i.e., Synergy weights and control signals are unknown, so the overall problem is non-convex. Finding a global minimum for non-convex problems can be very challenging. There exist a few algorithms to implement the concept of NMF. Kim et al., adopted the alternating least square (ALS) method to address the problem of non-convexity [27]. ALS is a two-way optimization method that caters to the non-convexity by employing an iterative methodology, it is a block coordinate descent technique. To attain an optimal solution

ALS requires the sub-problems to have a unique solution. However, the property does not hold as the sub-problems are convex but not strictly convex [28]. Therefore, to attain optimal decomposition using the ALS method this paper recommends the use of optimization constraints, making the problem overall a bounded optimization function. The penalty function can be based on $l_1 - norm$ known as Sparsity constraint and $l_2 - norm$, the Euclidean distance [29]. For the selection of the correct regularization constraint, the model in question must be considered. For bio-signals, the sEMG matrix cannot always be considered sparse; however, the control signals can always be assumed to be uncorrelated. Therefore, in order to provide a better solution and faster convergence using the ALS algorithm, this paper proposes the use of standard Tikhonov ($l_2 - norm$) constraint. The use of $l_2 - norm$ as penalty function will impose boundness as well as smoothness on the solution [30]; this approach is referred to as regularized NMF. To the best of our knowledge, regularized NMF has not been utilized for bio-signal applications in literature so far.

Regularized NMF algorithm

Five main nerves carry signals from the spinal cord to the human arm, different synergistic combinations of these nerves are involved in activation of different DOFs [31]. The information carried by the combination of nerves is decoded and transmitted to the group of muscle fibers, which is, later, picked up by the sEMG electrode. To attain maximum information, P number of electrodes are placed on the arm in a circular arrangement, targeting different muscles; the resulting sEMG signals matrix (Y) thus obtained has a dimension [L × P]. To achieve maximum information addressing different muscles of the arm, the number of electrode channels are always kept more than the number of nerve-channels involved, i.e., P > 5; therefore, the sEMG observer matrix has a greater dimensionality than the rank (r) of the matrix. To obtain a synergy matrix that has rank 'r ' with low error, the ALS low-rank algorithm proposed by [17] is incorporated in a modified manner to satisfy the regularized NMF penalty as well as fulfill bio-signals estimation requirements. Let the estimated low rank sEMG signals matrix be $\hat{Y} \in Y_r \left(Y_r \subset \left\{ Y \in \mathbb{R}^{[L \times P]} : rank(Y) = rank(Y_r) = r \right\} \right)$, that is defined as (eq. 8).

$$\hat{Y} = \genfrac{}{}{0pt}{}{argmin}{Y \in Y_r} ||Y - S\phi(t)||_2 \tag{8}$$

For the implementation of $l_2 - norm$, two regularization coefficients and two regularization matrices are incorporated, i.e., α_S and α_ϕ, and L_S and L_ϕ for synergy and control signals, respectively. The use of regularization parameters enforces maximum uncorrelatedness of the synergies and the control signals. While L_S and L_ϕ, are used to enforce application dependent characteristics, in the proposed case the regularization matrices are initialized as the trace elements, i.e., $L_S = trace\{S^T E S\}$ and $L_\phi = trace\{\phi(t)^T E \phi(t)\}$ [30]. The use of regularization coefficients and regularization matrices together provides a good fit leading to an optimum mean square error.

$$\hat{Y} = \genfrac{}{}{0pt}{}{argmin}{Y \in Y_r} ||Y - S\phi(t)||_2^2 + \alpha_S ||SL_S||_2^2 + \alpha_S \left\| L_\phi \phi(t) \right\|_2^2 \tag{9}$$

$$subject\ to\ S_{l,j}, \phi_{j,l}(t) \geq 0; l = 1, \dots, L \ \&j = 1, \dots, J$$

For computational efficiency and convergence, the regularization terms α_S and α_ϕ are defined as decreasing exponentials, i.e., $\alpha_S^m = \alpha_\phi^m = \beta \alpha^{m-1}; 0 < \beta < 1$ and $\alpha = \sigma_{rest\ region}^2$; where $'m'$ is the iteration number and $\sigma_{rest\ region}^2$ is the variance when the hand is at rest.

Results

To implement the proposed model, the rest (inactive) regions of the muscles were separated from active regions using an adaptive Teager Kaiser energy operator-based algorithm as proposed in previous work [3], which marked muscle's activation region, i.e., onset and offset points. Each detected pair of onset offset corresponded to one repetition of a movement. RMS was calculated for each repetition using a sliding window of size, 'T_a' with an overlap between two consecutive windows of length, 'T_{ol}'. After extensive analysis based on the accuracy of correct movement detection and time required to process the sEMG data, the duration of 'T_a' was fixed to 100 ms and 'T_{ol}' to 25 ms. Further discussion is presented in the discussion section. To estimate the rank correctly, the number of synergies was iteratively varied from 1 to 6, the VAF test was performed on the data of all the participants. The basic VAF formulation is provided in eq. (10). There exist different VAF based selection algorithms in the literature [33,34]; this paper utilizes a slight variation of the procedure followed by [33]. Fig. 4 provides VAF verses a few synergy curve tests conducted with two randomly selected repetitions of each movement from each participant's database. From (fig. 4) it is observed that the most optimal rank is between 2 to 4 synergies, as the knee curve resides in this region. When the number of synergies is less than or equal to 2, we observe a very low VAF indicating loss of information. While maximum accuracy is reached for 4 synergies and there is no significant improvement in VAF by increasing synergies further; a clear sign that 4 synergies are providing sufficient information catering all target movements. Therefore, further analyses will be carried out for 3rd and 4th rank synergy matrices only.

$$VAF = \left(1 - \frac{var(Y - \hat{Y})}{var(Y)} \right) \times 100\% \tag{10}$$

Figure 6 The result of Variance Accounted For (VAF) for rank estimation is presented. VAF percentage vs. the number of synergies are plotted. Each color dot represents average VAF for all 18 movements targeting single as well as double active DOFs for all 12 participants. The minimum and maximum VAF values are highlighted with a black straight line. It is evident that four synergies were able to explain more than 90% of the variance in the data as well as the results are more concentrated towards the average value.

For a fair comparison the proposed methodology is compared with other variants of NMF family as well as other synergy models, i.e., classic NMF(P) [35], ALS based NMF [36], Sparse

NMF (SNMF) [18,37], pICA, and a hybrid model comprised of pICA and LDA [9]. All the experiments were performed using the Matlab 2016a version on a Core i-7 (2.4 GHz) processor. A detail of the computational cost is discussed at the end of this section.
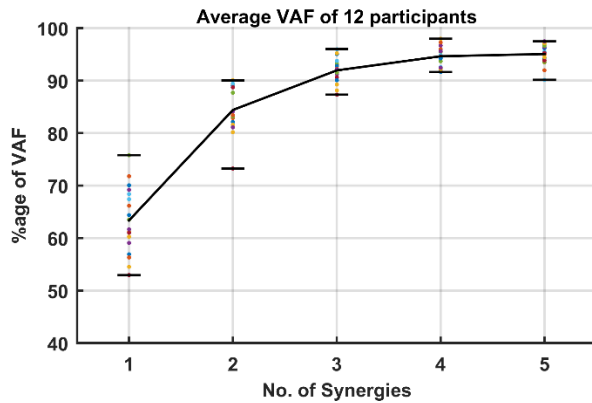

Figure 7 Variance Accounted For (VAF) for rank estimation.

Efficient human-machine interface systems are more accurate for multi-functional operations and should have a fast response. It is a common observation that when an analysis window is large, better task discrimination results are achieved [6,9,25]. However, longer the size of the analysis window, the greater is the computational time and slower the response. Hence, there is always a compromise between the length of the analysis window and the accuracy performance. To choose an acceptable window length without compromising on the performance of the algorithm we provide a comparison on the bases of percentage accuracy and computational delay defined as $D = \frac{1}{2}T_a + \frac{1}{2}T_{ol} + T_{proc}$ [17]. According to the study conducted by Farell et al., for fast prehensor a speed of 36.7 cm/sec is observed while for slower processors it is 10.2 cm/sec resulting in a delay range of 138 msec to 172 msec. However, after extensive study and controller accuracy performance test, Farell et al., concluded that an optimal delay range for a controller was observed between 100-120 msec [17]. The Hybrid model leads to maximum latency both for 1 and 2 DOF (Fig. (5)). When probed in-depth, it is observed that the higher computational time is due to the use of PR based classifier where the Hudgin's parameter calculation followed by LDA increases the processing time by 43.2 msec, leading to a total delay of 116 msec for 1 DOF that increases to 292 msec for 2 DOF. We also estimated the computational time of the pICA for the given model. The pICA synergy tracking time is almost as low as that of NMF; however, the window length as per the recommendation of [9] makes the overall delay more pronounced. For a fair comparison in our earlier paper [20], the analysis window size for the Hybrid model was decreased to 100 msec for 1 DOF. With the decrease in the window lengths, the temporal resolution decreases to a limit that it deteriorates the performance of the algorithm. Therefore, in this paper, the Hybrid model and pICA are implemented as per the recommended settings.
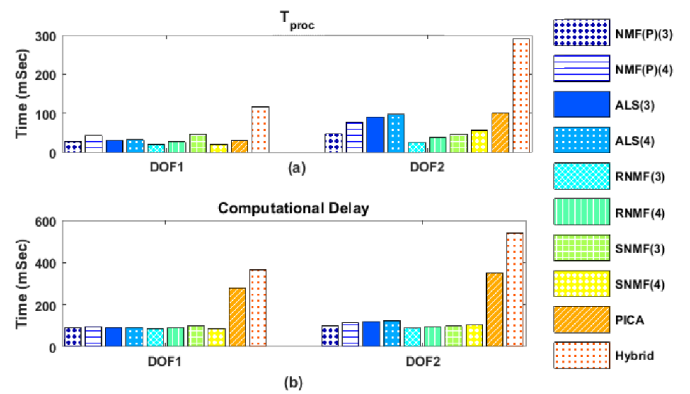

Figure 8 (a) a comparison of processing time of different algorithms for synergy estimation using NMF (b) the computational delay analysis for different techniques.

Figure 9 (a) Provides a comparison of processing time of different algorithms for synergy estimation using NMF and its variants as well as probabilistic ICA while the bars at the rightmost presents Hybrid model (in case of 1 and 2 DOF results). (b) provides the computational delay analysis for different techniques using formula $D = \frac{1}{2}T_a + \frac{1}{2}T_{ol} + T_{proc}$.

Discussion

The database comprises of the twelve healthy participants performing eighteen different movements. The result of the VAF test performed on two randomly selected trials of all eighteen movements (i.e., 1 and 2-DOF) from all twelve participants is represented in fig. 4. For the proposed algorithm two different synergies matrices with rank, r = 3 and r = 4 are compared based on processing time (T_{proc}) as well as total computational cost (D) with other techniques available in the literature (as discussed in the previous section). Fig. 5a demonstrates that for single active DOF minimum processing time is consumed by 3rd order regularized NMF and 4th order SNMF (i.e., 20 msec each). While the second-fastest performer is 4th order regularized NMF with a processing time of 27 msec. When the number of simultaneous active DOF is increased, the 3rd order regularized NMF is still the fastest among all the algorithms (26 msec) but the SNMF performance deteriorates reaching a 56 msec processing time. On the other hand, 4th order R-NMF provides better processing time for both 1 and 2 DOFs, i.e., 27 msec and 38 msec, respectively. Based on the comparison of computational time as well as the average VAF score (i.e. an improvement by 7%), this paper recommends the use of the 4th order synergy matrix, i.e., r = 4.

Fig. 5b presents the total computational delay (D) for various synergy as well as hybrid algorithms. The synergy group comprises of several variants of NMF as well as pICA, whereas the hybrid approach used pICA followed by LDA based classifier. The computational delay is based on the analysis and overlap window lengths, as well as the processing time. For the comparison with NMF based approaches, this paper uses $T_a = 100\ msec$ while $T_{ol} = 25\ msec$; whereas for comparison with pICA and Hybrid approach recommended values are followed [35], i.e., $T_a = T_{ol} = 250\ msec$.
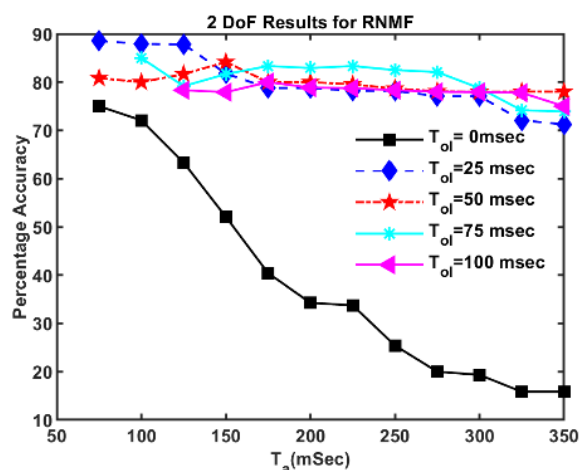
Figure 10 A comparison for movement discrimination accuracy for R-NMF.

Figure 11 A comparison for movement discrimination accuracy for R-NMF is presented with different sizes of the analysis window length (T_a) and length of overlap between two consecutive windows (T_{ol}).

Fig. 6 provides an insight into the performance of 4th order regularized NMF when multiple DOF are activated simultaneously. The algorithm is compared for different values of analysis window size, 'T_a', and the size of the overlap between two consecutive analysis windows, 'T_{ol}'. It is observed that the analysis window provides the best performance with $75 \; msec \leq T_a \leq 150 \; msec$. As far as the size of overlap is concerned, better performance is observed for $T_{ol} = 50 \; msec$; however, for the desired range of 'T_a' the best choice is to keep $T_{ol} = 25 \; msec$.
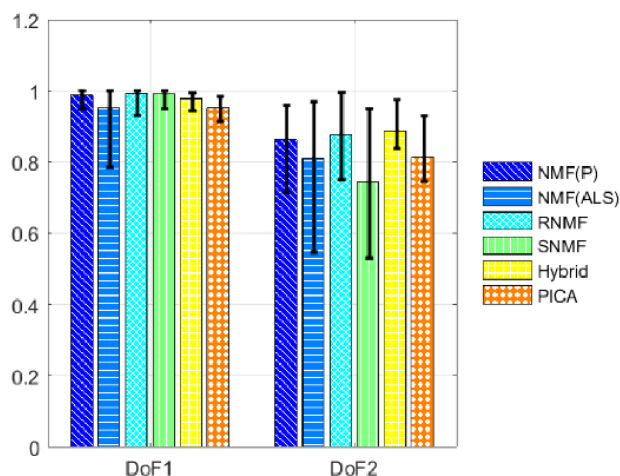

Figure 12 NMF: non-negative matrix factorization; ALS: alternating least-square; ICA: independent component analysis; Accuracy rates (bars) with deviation from the mean (error bars).

Fig. 7 presents movement discrimination accuracy of different algorithms for single as well as multiple active DOF. The ALS based NMF algorithm, although being fast as compared to the classic NMF algorithm, suffers from the complexity of sub-problems; therefore, it is the least performer when it comes to synergy estimation and respective task discrimination. The

addition of penalty functions such as sparseness and regularization constraint to ALS improves the results considerably. In the case of a single active DOF constrained ALS improves the performance by 4 to 5%; however, it is observed that in the case of 2 DOF the sparseness constraint is not able to discriminate multiple active DOF simultaneously. Whereas the regularization constraint handles the problem easily and provides considerably better results. In terms of accuracy for the case of multiple active DOF, the proposed model is the second-best to the Hybrid model, but when considering both the computational cost as well as the discrimination performance, regularized NMF outperforms all other options.

Conclusion

Synergistic weight estimation plays a vital role in the field of neurorehabilitation, where diagnosis of the neural muscular activation of different limbs is an emerging area as well as in the field of assistive devices control. To the best of the authors information regularized NMF has not been previously used for bio-signal decomposition. This paper investigates the use of regularization penalty function for the improvement of muscle synergies. The imposition of regularization constraint with the ALS algorithm helps in attaining optimal and fast solutions for the NMF-based system, resulting in minimum time and better task discrimination. The proposed algorithm provides almost identical results as those of the Hybrid model for multiple active DOF but with quite low complexity in terms of computational cost. Among the NMF family, the proposed methodology performs the best in terms of computation analysis as well as accuracy performance. Furthermore, the proposed method does not require isolated triggering of individual DOFs. The authors are looking forward to use the proposed algorithm for estimation of muscle synergies in amputees and stroke patients for better diagnosis of the neural muscular changes and future applications. In future the author aims to perform targets assessment test for online evaluation.

References

1. Farina, D and Jiang, N and Rehbaum, H and Holobar, A and Grainmann,B and Dietl, H and Aszmann, O. The extraction of neural information from the surface EMG for the control of upper limb prosthesis: Emerging avenues and challenges. IEEE transaction on Neural Systems and Rehabilitation Engineering; 2014: 22(4): p. 797-809.
2. Adewuyi, A A and Hargrove, L J and Kuiken, T A. Evaluating EMG feature and classifier selection for application to partial hand prosthesis. Frontiers in Neurorobotics; 2016:10(15): p. 1-25.
3. Gokgoz, E and Subasi, A. Comparison of decision tree algorithms for EMG signal classification using DWT. Journal of Biomedical Signal Processing and Control; 2015: 18: p.138-144.
4. Al-Timemy,A H and Rami, N and Khushaba and Bugmann, G and Escudero, J. Improving the Performance Against Force Variation of EMG Controlled Multifunctional Upper Limb Prostheses for Transradial

Amputees. IEEE Transactions on Neural Systems and Rehabilitation Engineering; 2015: 24(6): p. 650 - 661.

5. Chen, X and Yuan, Y and Cao, S and Zhang, X and Chen, X. A SEMG-Force Estimation Framework Based on a Fast Orthogonal Search Method Coupled with Factorization Algorithms. Sensors; 2018: 18(17): p. 22-38.

6. Ebied, A and Lang, EK and Spyrou, L and Escudero, J. Evaluation of matrix factorization approaches for muscle synergy extraction. Medical, Engineering & Physics; 2018: 57: p.51-60.

7. Farrell, T and Weir, R F. A comparison of the effects of electrode implantation and targeting on pattern classification accuracy for prosthesis control. IEEE Transactions onBiomedical Engineering; 2008: 55(9): p. 2198-211.

8. S Israely and G Leisman and C MAchluf and T Shnitzer and E Carmeli. Direction modulation of muscle synergies in a hand-reaching task. IEEE Transaction on Neural systems and Rehabilitation engineering; 2017: 25(12): p. 2427-2439.

9. Rasool, G. and Iqbal, K. and Bouaynaya, N. and White, G. Real-time task discrimination for myoelectric control employing task-specific muscle synergies. IEEE Transaction on Neural Systems and Rehabilitation Engineering;2016 :24(1): p. 98-108.

10. S Zhang and X Zhang and S Cao and X Gao and X Chen and P Zhou. Myoelectric Pattern Recognition based on muscle synergy for simultaneous control of Dexterous finger movement. IEEE Transaction of Human-Machine systems; 2017: 47(4): p. 576 - 582.

11. D Farina and F Negro. Accessing the Neural Drive to Muscle and Translation to Neurorehabilitation Technologies. IEEE Review in Biomedical Engineering, ;2012: 5: p. 3-15.

12. I Delis and P M Hilt and T Pozzo and S Panzeri. Deciphering the functional role of spatial and temporal muscle synergies in whole-body movements. Scientific Reports; 2018:8(1038): p. (1-16).

13. A dAvella and F Iacquaniti. Control of reaching movements by muscle synergy combination. Frontiers in Computational neuroscience; 2013:7(42): p. 1-7.

14. N Jiang and K B Englehart and P A Parker. Extracting Simultaneous and Proportional Neural Control Information for Multiple-DOF Prostheses From the Surface Electromyographic Signal. IEEE Transaction On Biomedical Engineering, ;2008: 56(4): p. 1070-1080.

15. M Santello and M Flanders and J Soechting. Postural hand synergies for tool use, . Journal of Neuroscience; 1998:18(23): p. 10105-10115.

16. Hahne, J M and Dahne, S and Hwang, H J and Muller, K R and Parra. L C. Concurrent adaptation of human and machine improves simultaneous and proportional myoelectric control. IEEE Transactions on Neural Systems and Rehabilitation Engineering; 2015: 23(4): p. 618-627.

17. Farrell, Todd R. and Weir, Richard F.The Optimal Controller Delay for Myoelectric Prostheses. IEEE Transactions on Neural Systems and Rehabilitation Engineering; 2007: 15(1): p. 111-118.

18. C Lin and B Wang and N Jiang and D Farina. Robust extraction of basis functions for simultaneous and proportional myoelectric control via sparse non-negative matrix factorization. Journal of Neural Engineering; 2018: 15: 26017(9pp).

19. Hugelier, S and Piqueras, S and Bedia, C and Juan, A D and Ruckebusch, C. Application of a sparseness constraint in multivariate curve resolution Alternating least squares. Analytica Chimica Acta; 2018: 1000: p. 100-108.

20. R. Bahadur and S. u. Rehman and S. Khattak. Synergy Estimation for Myoelectric Control Using Regularized NMF. 41st Annual International Conference of the IEEE Engineering in Medicine and Biology Society (EMBC); 2019: p. 2649-2652.

21. Negro, F and Muceli, S and Castronovo, AM and Holobar, A and Farina, D. Multi-channel intramuscular and surface EMG decomposition by convolutive blind source separation. Journal of Neural Engineering; 2016: 13: p. 1-17.

22. Todorov, E. Stochastic optimal control and estimation methods adapted to the noise characteristics of the sensorimotor system. Neural Computation; 2005: 17(5): p. 1084-1108.

23. Naik, G R and Al-Timemy, AH and Nguyen, H T. Transradial Amputee Gesture Classification Using an Optimal Number of sEMG Sensors: An Approach Using ICA Clustering. IEEE Transactions on Neural Systems and Rehabilitation Engineering; 2015:24(8): p. 837- 846.

24. Staudenmann, D and Dafiertshofer, A and Kingma, I and Stegeman, D F and Dieen, J H. Independent Component Analysis of High-Density Electromyography in Muscle Force Estimation. IEEE Transactions on Biomedical Engineering;2007: 54(4): p. 751-754.

25. Antuvan, C.W. and Bisio, F and Marini,F and Yen,S.C. and Cambria, E and Masia, L. Role of muscle synergies in real-time classification of Upper Limb motions using Extreme Learning Machines. Journal of Neuro Engineering and Rehabilitation; 2016: 13(1): p.76-91.

26. Jiang, N and Rehbaum, H and Vujaklija, I and Graimann, B and Farina, D. Intuitive, online, simultaneous, and proportional Myo-electric control over two degrees-of-freedom in Upper Limb Amputees. IEEE Transactions on Neural Systems and Rehabilitation Engineering; 2014: 22(3): 501-510.

27. Kim, J and Park, H. Toward Faster Nonnegative Matrix Factorization: A New Algorithm and Comparisons. IEEE International Conference on Data Mining; 2008: p. 353-362.

28. A. M. S. Ang and N. Gillis. Algorithms and Comparisons of Nonnegative matrix factorization with Volume Regularization for Hyperspectral Unmixing. Circuits, Systems, and Signal Processing;2016: 35(12): p.4532-4549.

29. Shang, R and Liu, C and Meng, Y. Nonnegative Matrix Factorization with Rank Regularization and Hard Constraint. Neural Computation; 2017: 29(9): p. 2553-2579.

30. Cichocki, A. and Zdunek, R. and Phan, A. H. and Amari, S. Alternating Least Squares and Related Algorithms for NMF and SCA Problems.. Non-negative matrix and tensor factorizations: Application To exploratory multi-way data analysis and blind source separation; 2009: p. 203-266.

31. Inner Body: Nerves of the Arm and Hand. https://www.innerbody.com/anatomy/nervous/arm-hand; 2019.

32. Bahadur, R and Rehman, S U; A Robust and Adaptive Algorithm for Real-time Muscle Activity Interval Detection using EMG Signals. Proceedings of the 11th International Joint Conference on Biomedical Engineering Systems and Technologies;2018: 4: p.89-96.

33. Cheung, V.C. and Piron, L. and Agostini, M. and Silvoni, S. and Turolla, A. and Bizzi, E.. Stability of muscle synergies for voluntary actions after cortical stroke in humans. Proceedings of the National Academy of Sciences of the USA; 2009: 106(46); p. 19563-19568.

34. Frere, J. and Hug, F.Between-subject variability of muscle synergies during a complex motor skill. Frontiers in Computational Neuroscience; 2012:6(99): p.1-13.

35. Lee, D D and Seung, H S. Algorithms for Non-negative matrix factorization. Advances in Neural Information Processing Systems; 2001: 13: p. 556-562.

36. Kim, J and Park, H. Fast Nonnegative Matrix Factorization: An Active-set-like Method And Comparisons. SIAM Journal on Scientific Computing; 2011: 33(6): p.3261-3281.

37. Kim, H and Park, H. Sparse Non-negative Matrix Factorizations via Alternating Non-negativity-constrained Least Squares for Microarray Data Analysis. Bioinformatics; 2007: 23(12): p. 1495-1502.